ACS OMEGA

http://pubs.acs.org/journal/acsodf

Article

Exploring the Inclusion Complex of an Anticancer Drug with β-Cyclodextrin for Reducing Cytotoxicity Toward the Normal Human Cell Line by an Experimental and Computational Approach

Published as part of the ACS Omega virtual special issue "Phytochemistry".

Antara Sharma, Pranish Bomzan, Niloy Roy, Vikas Kumar Dakua, Kanak Roy, Abhinath Barman, Rabindra Dey, Abhijit Chhetri, Rajani Dewan, Ankita Dutta, Anoop Kumar, and Mahendra Nath Roy*

Cite This: *ACS Omega* 2023, 8, 29388−29400

Read Online

ACCESS | Metrics & More | Article Recommendations | Supporting Information

ABSTRACT: The toxicity of any drug against normal cells is a health hazard for all humans. At present, health and disease researchers from all over the world are trying to synthesize designer drugs with diminished toxicity and side effects. The purpose of the present study is to enhance the bioavailability and biocompatibility of gemcitabine (GEM) by decreasing its toxicity and reducing deamination during drug delivery by incorporating it inside the hydrophobic cavity of β-cyclodextrin (β-CD) without affecting the drug ability of the parent compound (GEM). The newly synthesized inclusion complex (IC) was characterized by different physical and spectroscopic techniques, thereby confirming the successful incorporation of the GEM molecule into the nanocage of β-CD. The molecular docking study revealed the orientation of the GEM molecule into the β-CD cavity (−5.40 kcal/mol) to be stably posed for ligand binding. Photostability studies confirmed that the inclusion of GEM using β-CD could lead to better stabilization of GEM (≥96%) for further optical and clinical applications. IC (GEM-β-CD) and GEM exhibited effective antibacterial and antiproliferative activities without being metabolized in a dose-dependent manner. The CT-DNA analysis showed sufficiently strong IC (GEM-β-CD) binding (K_a = 8.1575 × 10^{10}), and this interaction suggests that IC (GEM-β-CD) may possibly exert its biological effects by targeting nucleic acids in the host cell. The newly synthesized biologically active IC (GEM-β-CD), a derivative of GEM, has pharmaceutical development potentiality.

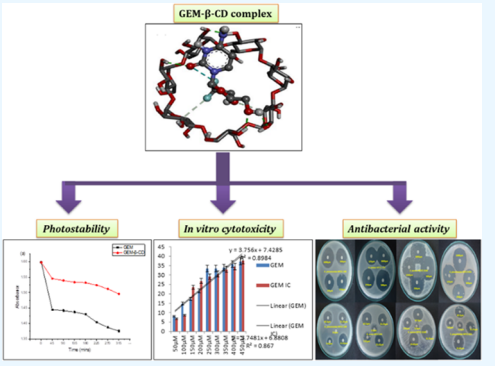

1. INTRODUCTION

Enhancement in the utility of drugs is of utmost priority among researchers in the present world. One way to achieve it is by minimizing the consequences due to the side effects of the drug. Certainly, it is important to develop methods or to modify the existing procedures to increase the bioavailability of drug molecules as more than half of the population around the globe suffers from various diseases caused by bacterial, fungal, and microbial infections. However, with the success of available vaccines and antibiotics, the mortality rate due to such diseases has been brought down drastically. Along with this, the current improvement in primary and secondary precautions for cardiovascular diseases has made it clear now that cancer is actually the first or second cause of premature death in more than 180 countries in recent times.[1] In the year 2008, over 12 million people were diagnosed globally with cancer and the number has been increasing rapidly till date.[2] During the last few decades, many chemotherapeutic drugs have shown significant activity against different types of human carcinoma. Among various chemotherapy agents, gemcitabine (2′-deoxy-2′,2′-difluorocytidine) is found to be one of the most promising and effective agents against different types of cancers.[3−5] Gemcitabine (GEM) is a chemotherapeutic drug with huge potential for treatment of different types of cancers.[6−8] It is an anticancer drug with promising clinical application, but has limited effectiveness because of its toxicity and inactiveness in serum. It is a leading drug for pancreatic cancer treatment but has limited efficiency due to the fast deamination of N-4 amine, thus making it inactive in blood plasma.[9−11] A great variety of gemcitabine prodrugs have been investigated and developed to protect GEM from deamination; still, the clinical application of such prodrugs has been restricted due to their toxicity.[12−14] When gemcitabine is combined with the FOLFIRINOX, the regimen has been found to increase its activity even in case of

Received: April 26, 2023
Accepted: July 25, 2023
Published: August 3, 2023

https://doi.org/10.1021/acsomega.3c02783
ACS Omega 2023, 8, 29388−29400

metastatic pancreatic cancer, but also sufficiently increases the toxic effect manifold, thus leading to the patient being in an adverse condition.[15−17] Therefore, a great deal of research has increasingly been carried out in the past few decades to improve the drug delivery system of GEM.[17−20] A phase III clinical trial of gemcitabine in combination with erlotinib reported a slight improvement in overall survival (6.24 vs 5.91 months).[15,16,21−28] Likewise, the phase II trial of ACOSOG Z5041 showed positive results when gemcitabine was given along with erlotinib.[11] However, the scattered or arbitrary medical trial LAP07 reported that the combination of drug GEM failed to enhance survival despite patient consent.[12] The multicenter scattered phase III trial CONKO-005 disclosed almost no change in the universal survival from pancreatic cancer. In fact, most of the medical trials have highlighted the adverse effects due to the use of the combination chemotherapeutic drug.[8−14] Encapsulating cancer drugs within nanoparticles (NPs) can lessen their side effects through selected delivery and guided release. The U.S. Food and Drug Administration (FDA) and the European Medicines Evaluation Agency (EMEA) have approved polylactic-*co*-glycolic acid (PLGA) NPs as drug delivery systems. PLGA has various supreme properties such as surface tunability, biocompatibility, biodegradability, and controlled release.[15−17] Jaidev et al. evaluated the biophysical and photophysical properties of gemcitabine-loaded PLGA nanocavities in vitro,[18] and Aggarwal et al. prepared PLGA-poly(ethylene glycol) (PEG) NPs layered with the anti-EGFR monoclonal antibody for sustained delivery to malignant cells.[19] However, one limitation these NPs suffer is that they are acknowledged by the reticuloendothelial system as foreign particles and are subsequently partly removed by the immune cells.[20] Recently, camouflaged NPs have been developed and investigated for the sustained release of drugs. Although a great variety of work has been reported, this technique has not been standardized for a large population. Again, cost effectiveness is also a serious concern as half of the world's population suffering badly from cancer come from underdeveloped nations.[1,2] Furthermore, the treatment of cancer with cancer drugs may cause the additional difficulty of eroding the immune system and in some cases may even lead to immunodeficiency. Therefore, cancer patients undergoing chemotherapy treatment are more susceptible to acquire different kinds of microbial infections. According to various reports, microbial infections are among the major reasons of mortality among malignant patients.[4] Thus, there is an absolute need for a drug that has anticancer properties along with antibacterial properties. Gemcitabine fits very well in this criterion.[21−26] However, the rapid decrease in gemcitabine concentration in blood plasma requires excess doses of the drug in chemotherapy treatment. Also, as mentioned above, there is an urgent requirement to develop a delivery system that can enhance its sustained release with decreased rate of deamination alongside retaining/enhancing its antimicrobial property. A drug with such potential application could decrease the secondary effect and increase the probability of rapid recovery and ultimately the survival of cancer patients. Hence, considering all of the above conditions, we have synthesized an inclusion complex of GEM with β-cyclodextrin (β-CD) as a vast investigation on various drugs' encapsulation by cyclodextrins has already been done in the past few decades.[31−34] Among the variety of host molecules used for the purpose, the common compounds are cyclodextrins, cucurbiturils, and calixarenes. Cyclodextrins (CDs) are known for their ability of sustained release of drug molecules by forming an inclusion complex, thus leading to the increased bioavailability and biocompatibility of the compound.[29−31] CDs are also found to enhance the chemical stability by shielding the drug and increasing solubility.[29−33] CDs are cyclic oligosaccharides with six (α-CD), seven (β-CD), and eight (γ-CD) glucopyranose units, joined by α-1,4-linkages. They are endowed with a hydrophobic cavity internally and a hydrophilic surface externally. The hydrophobic part of the drug gets encapsulated partially/completely into the hydrophobic cavity.[34] Therefore, CDs have various applications in diverse fields like drug delivery, pharmaceuticals, textile industry, pesticides, supramolecular host-guest chemistry, food stuffs, molecular encapsulation, toilet articles etc.[30−33]

Here we report for the first time the incorporation of gemcitabine (GEM), an approved anticancer drug molecule, within the cavity of β-CD in aqueous medium. As cancer is the most significant reason for death all over the world, anticancer drugs find a very important place in the past, present, and future research. Thus, it is of great significance to enhance the biocompatibility of such molecules by the available nontoxic methods. In the present work we have tried to enhance/retain the bioavailability of GEM by decreasing its toxicity and increasing its photostability toward healthy cells through encapsulation with β-CD. Job's plot from UV−visible studies has shown 1:1 encapsulation. We employed the absorption (UV−visible) spectroscopic technique to calculate the association constant along with thermodynamic parameters. The GEM-β-CD IC thus prepared was characterized by Fourier transform infrared (FT-IR) spectroscopy, high-resolution mass spectrometry (HRMS), ^{1}H nuclear magnetic resonance (NMR) spectroscopy, X-ray diffraction technique, and scanning electron microscopy (SEM). Molecular docking study was done to understand the plausible interaction between GEM and β-CD. Antibacterial study against a great variety of pathogens was also carried out to investigate the advantages of GEM encapsulation in the biocompatibility of GEM. Photostability study was also carried out to understand the further application of encapsulated GEM.

2. EXPERIMENTAL SECTION

2.1. Materials. Gemcitabine (purity >98%) and β-cyclodextrin with purity 98% were acquired from TCI chemicals and Sigma-Aldrich, India, respectively, and further analysis was carried out as received. Human cell lines were procured from the National Centre for Cell Science, Pune, India. The medium and other materials used for animal cells were procured from Hi-media Laboratory Pvt. Ltd. MTT was bought from Hi-media, India, and DCDF dye was procured from Sigma India Pvt. Ltd. All materials and solvents utilized in the study were of analytical grade and were obtained from Hi-media, India; Sisco Research Laboratories, India; TCI Chemicals, India; Sigma India Pvt. Ltd.; and E. Merck, Germany.

2.2. Methods. The Agilent 8453 UV−vis spectrophotometer was utilized to record the UV−visible spectra. The temperature of the cell was kept fixed by an automated thermostat.

The Bruker Avance 300 MHz NMR spectrometer was used for ^{1}H-NMR measurements with D_2O as a solvent at 298.15 K.

HRMS spectra were recorded with positive-mode electrospray ionization in high-resolution Q-TOF instrument.

The Perkin-Elmer FT-IR spectrometer was used to measure the IR spectra using the KBr disk method at room temperature.

https://doi.org/10.1021/acsomega.3c02783
ACS Omega 2023, 8, 29388−29400

The Bruker D8 advance powder X-ray diffractometer was used to record powder XRD experiments. A JSM-6360 scanning electron microscope (SEM) was used for the surface morphological analysis.

2.3. Preparation of the Inclusion Complex. The solid inclusion complex (IC) (GEM-β-CD) was synthesized by employing the co-precipitation method.[35] GEM and β-CD were mixed in 1:1 molar ratio; 1.0 mmol β-CD and GEM were separately dissolved in 20 and 25 mL of distilled water, and then GEM solution was added dropwise to the β-CD solution with constant stirring. The solution was continuously stirred for 48 h at 45 °C. After this, the solution was made concentrated by slow evaporation; the thus-obtained solid mass was then filtered and washed thoroughly with ethanol and water simultaneously for a couple of times to remove the unreacted β-CD and GEM. Thereafter, the purified mass was desiccated in an oven at 50 °C for 20 h. Ultimately, the solid IC powder was received and kept in vacuum desiccators for additional advanced analysis.

2.4. Absorption Spectral Titrations. The UV−visible spectral titration method[36,37] was employed to study the inclusion complex IC (GEM-β-CD) formation of β-CD with drug GEM in aqueous solution.[46,47] A 1.0 mL (80 μM) solution of GEM was taken in a cuvette and then, varied concentrations ranging from 1.0 to 5.0 mM of a 1.0 mL β-CD solution was added to it, such that the concentration of GEM was 40 μM for the (GEM) + (β-CD) system in all cases.

2.5. Job's Method for Stoichiometric Determination of the Inclusion Complex. The best method available to resolve the stoichiometry of the host and guest in supramolecular chemistry is Job's method, commonly known as the continuous variation method. This method was employed here using the UV−visible spectroscopic technique.[35−37] Job plot was derived by plotting $\Delta A \times R$ versus R (where R = [GEM]/([GEM] + [β-CD] and ΔA) denotes the difference in absorbance of GEM in the absence and presence of β-CD). A series of solutions of GEM and β-CD were prepared in such a way that the total concentration, [GEM] + [CD], remains constant while the mole fraction of GEM varies in the range of 0−1 at 298.15 K (Tables S1). The maxima on the plot indicates the stoichiometry of the prepared inclusion complex and in the present work, it is observed at R = 0.5, clearly indicating the 1:1 stoichiometric ratio of IC (Figure 1).[34] Absorbance values were evaluated at λ_{max} = 268 nm.

2.6. Preparation of 3D Structures of GEM and β-CD. The three-dimensional structure of GEM was obtained from PubChem website (http://pubchem.ncbi.nlm.nih.gov). β-CD was obtained with deposit number CCDC ID: 762697 from the Cambridge Crystal Data Centre (CCDC).[38] The missing hydrogen atoms and atomic charges were added to β-CD as well as GEM, and the structures were optimized using the DFT-B3LYP method with Gaussian 09 software prior to carrying out the computational studies.[39]

2.7. Molecular Docking Study. Molecular docking is a computational method that is used to predict the preferable binding mode of a guest within a host.[40] An established docking protocol for a host-guest system implemented in PyRx was applied.[41] Prior to docking, all PDB files are converted into PDBQT format, and atomic coordinates were generated employing PyRx docking software. The grid box center values were set as center_x = 8.2006, center_y = 24.1273, and center_z = 1.2165, and dimension values as size_x = 19.3813, size_y = 19.2330, and size_z = 17.7765 for all of the three coordinates. The grid box size was made around the binding pocket of β-CD (receptor) such that GEM (ligand) moves freely in the space. According to the docking score, the lowest-energy conformer was selected and visualization was made using Discovery Studio Visualizer, v21.1.0.20298, BIOVIA.[42]

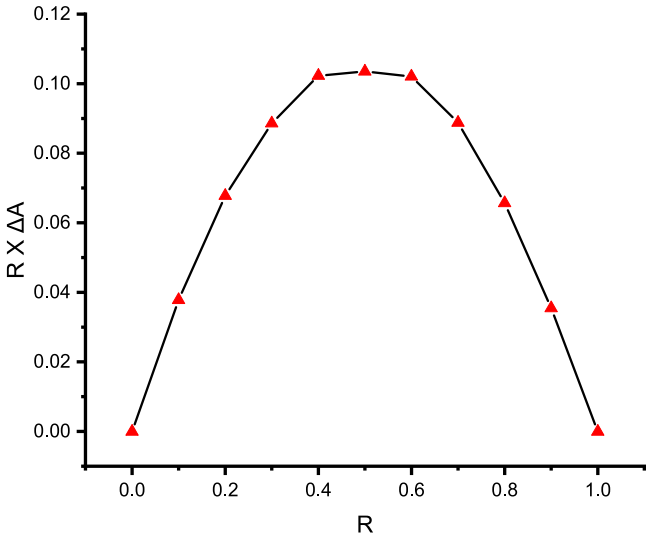

Figure 1. Job plot of the GEM-β-CD system at 298.15 K in H_2O at λ_{max} = 268 nm. ΔA = difference in absorbance of GEM in the absence and presence of β-CD, R = [GEM]/([GEM] + [β-CD]).

2.8. Antimicrobial Activity Assay. The potential antibacterial activity of GEM and the GEM-β-CD complex (IC) was determined by the classical disc diffusion approach as described by Bauer et al.[43] In the disc diffusion assay, a loopful of overnight-grown bacterial colony was inoculated into tryptone soya broth medium for exponential growth. After 6−8 h growth on a rotary shaker (150 rpm), the total cell concentration was adjusted approximately to 10^8/mL with sterile saline, and these cultures were used for surface spreading using a sterile swab on sterile Mueller-Hinton agar plates. Both the test drugs were dissolved separately in the sterile double-distilled water, and stock solutions of the drug were sterilized using a 0.22 μm syringe filter. After 15 min, the plates were impregnated with sterile Whatman no. 1 filter paper discs (6.0 mm diam.) containing desired concentrations of the test drugs (the residual solvent was completely evaporated in the laminar air flow, and the discs were aseptically placed on the Mueller-Hinton agar surface). Discs with chloramphenicol 30 μg/mL were used as a positive control for antibacterial activity assay. After 24 h of incubation at 37 °C, the inhibitory activity of the test drugs was determined by measuring the zone of inhibition (ZOI in nearest mm), including disc diameter.

2.9. Cell Line Culture. The normal human cell line was used to study the cytotoxicity activity of GEM and the prepared inclusion complex (GEM-β-CD IC). The cell line was procured from Cell Repository, National Centre for Cell Sciences (NCCS), Pune, India. These cells were cultured to reach confluence in Dulbecco's Modified Eagle Medium (Ham F-12 culture medium) maintained at 37 °C in a humidified atmosphere in a 5% CO_2 incubator.

2.10. *In Vitro* Cell Viability Assay. The cell viability of GEM and the synthesized inclusion complex (IC GEM-β-CD) was assessed by the MTT assay, as described by Mosmann.[44] Human cells were trypsinized and aseptically collected, counted, and adjusted to a final concentration of 5×10^3 cells/well, to be inoculated on 96-well plates containing sterilized 100 μL of

https://doi.org/10.1021/acsomega.3c02783
ACS Omega 2023, 8, 29388−29400

DMEM (Dulbecco's Modified Eagle Medium) Ham F-12 culture medium. After 24 h of observation, the cells were treated with increasing concentrations (50−450 μM) of GEM and the inclusion complex (IC GEM-β-CD) for 48 h. Thereafter, before the incubation time, a 1:10 volume of MTT solution (5 mg/mL) was added to each well and incubated for the next 3 h in dark. Then the medium was cautiously separated and the formazan produced in the wells was solvated in 50 μL of isopropanol for homogeneous measurement; then, the plates were kept on a plate shaker for 3−5 min. The absorbance peak was measured at 600 nm using an ELISA (microplate) reader (SPECTRO starNano, Germany). For the control, Ham F-12 culture medium (pH 7.4) and Dulbecco's PBS were used in place of the tested compounds. The percentage of cell toxicity was calculated as $\{(U - T)/U \times 100\}$, where "U" is the mean optical density of control (untreated cells) and "T" is the mean optical density of the treated cells with different drug concentrations. All experiments were performed in three replicates ($n = 3$).

2.11. Statistical Analysis. All data furnished in this work are the mean ± SD of *in vitro* experiments recorded with three test samples. The analysis of variance technique was used to analyze the results for statistical measurements. A P value <0.05 was regarded as statistically important. All analytical tests were performed using Origin Pro 8.5 and SPSS software.

3. RESULTS AND DISCUSSION

3.1. Determination of the Stoichiometric Ratio of the Inclusion Complex by Job's Method. $\Delta A \times R$ against R was plotted to generate Job's plot (where ΔA is the change in the absorbance of GEM with and without β-CD), and $R = [\text{GEM}]/([\text{GEM}] + [\beta\text{-CD}])$. The maximum peak value of R on the plot confirms the stoichiometry of complexation. From Figure 1, the observed maximum value of $\Delta A \times R$ at $R = 0.5$ establishes that the inclusion complex of GEM with β-CD is formed with a stoichiometric ratio of 1:1.

3.2. Absorption Spectral Analysis. The tendency of GEM to bind with β-CD was determined through binding constant (K_a) measurement with the help of UV−visible spectroscopic analysis.[45] The continuous increase in GEM absorbance confirms the encapsulation of the drug into the hydrophobic β-CD cavity. A hyperchromic shift is observed because β-CD molecules capture the drug (GEM) molecule within its orifice to form the inclusion complex, thereby decreasing the polar environment around the GEM molecule.[46] The association constant (K_a) of IC at 298.15 K was computed from the variation in the absorbance (ΔA) of GEM (at λ_{max} = 268 nm) with the increasing CD concentration by applying Benesi-Hildebrand equation (Tables S2). By employing the Benesi-Hildebrand equation (eq 2), a double reciprocal plot was obtained for the 1:1 complex formation as follows

$$\frac{1}{\Delta A} = \frac{1}{\Delta\varepsilon[\text{GEM}]K_a}\frac{1}{[\text{CD}]} + \frac{1}{\Delta\varepsilon[\text{GEM}]} \quad (1)$$

The plot of $1/\Delta A$ against $1/[\text{CD}]$ (Figure S1) shows a good linear correlation [R^2 = 0.99691 for IC (GEM-β-CD)], indicating the 1:1 stoichiometry of the GEM-β-CD complex. The binding constant (K_a) for the 1:1 GEM-β-CD complex, evaluated from the Benesi-Hildebrand plot using eq 1, was calculated as 19.4×10^3 M^{-1} for IC (GEM-β-CD). In order to understand the encapsulation process between β-CD and GEM, the Gibb's free energy of binding (ΔG) was calculated with the help of the value of binding constant K_a at 298.15 K using eq 2.

$$\Delta G = -\text{RT} \ln K_a \quad (2)$$

The value of ΔG was −5.85 kcal/mol for the GEM-β-CD complex (IC) at 298.15 K, which confirms the encapsulation process is spontaneous.

3.3. ^{1}H-NMR Analysis. The mechanism of encapsulation of GEM into the β-CD cavity could be best analyzed by ^{1}H-NMR study. In this work, a detailed analysis was performed and the information thus obtained ascertains the successful complexation. Upon encapsulation of the drug molecule within the CD pocket, upfield chemical shifts were observed for both the guest and the CD protons. This is mainly due to mutual shielding between the drug molecule and β-CD, thus resulting in enclosure of the former by the electron density of β-CD.[47,48] β-CD has H-5 and H-3 hydrogen atoms inside the cavity, whereas the remaining H-4, H-2, and H-1 hydrogen atoms lie on the exterior side of the surface. Thus, H-5 is placed in the vicinity of the narrower rim, whereas H-3 lies near the wider rim (Figure S7). Here, encapsulation of GEM with β-CD was investigated through ^{1}H-NMR spectroscopy and various other spectroscopic techniques. The ^{1}H-NMR spectra of β-CD, GEM, and GEM-β-CD are displayed jointly in Figure S2 and the corresponding chemical shifts ($\Delta\delta$) are given in Table S3. After the inclusion of the drug, it is observed that the outer H-4, H-2, and H-1 protons of CD suffer very negligible changes in chemical shifts but the inner H-5 ($\Delta\delta = -0.07$) and H-3 ($\Delta\delta = -0.092$) protons in the GEM-β-CD system experience a relatively greater change in chemical shift, thus suggesting the successful insertion of GEM within the CD cavity (Figure S2). As observed in Figure S2, H-3 protons experienced a remarkable upfield shift as compared to H-5 protons (Tables S3); it is proposed that the encapsulation occurred through the wider rim of the CD cavity. A comparative ^{1}H-NMR analysis of GEM with the GEM-β-CD complex reveals the considerable upfield shift in values of H-e ($\Delta\delta = -0.05$) and H-f ($\Delta\delta = -0.06$) protons, whereas the H-a, H-c, and H-d protons suffer negligible shift (Tables S3). Again, H-b also shows a slight upfield shift ($\Delta\delta = -0.013$), indicating that H-b, H-e, and H-f protons are involved in interaction with the inner protons of β-CD during encapsulation (Figure S2 and Tables S3). These findings clearly suggest that β-CD cavity encapsulates the drug molecule (GEM) through the five-membered ring containing oxygen (GEM) from the wider side of the rim (Figure S7).

3.4. ESI-MS Studies. The stoichiometric ratio between the drug and β-CD in the solid GEM-β-CD inclusion complex was further verified using the well-known electrospray ionization mass spectroscopy method in a solution of methanol (ESI-MS).[49] The peaks at m/z values 1398.44 and 264.07 corresponding to the molecular ions $[\text{GEM} + \beta\text{-CD}]^+$ and $[\text{GEM}]^+$ (Figure S3) markedly indicate that the host-guest in the GEM-β-CD inclusion complex has 1:1 stoichiometric ratio, thus certifying the results deduced from Job's method.

3.5. Analysis of FT-IR Spectra. The synthesized solid inclusion complex was further inspected through a very important and conclusive FT-IR spectroscopic method. The noncovalent molecular interaction between the host and the guest during inclusion was fully supported by the FT-IR spectral analysis.[50] The inclusion phenomena led to changes in the peak intensity, shape, position, and also the disappearance of some peaks in the FT-IR spectra of both drug and the host, certainly due to the change in electron density in their vicinity.[51] The infrared spectra of β-CD, GEM, and GEM-β-CD complex are depicted in Figure 2 and their chemical bonds along with the

https://doi.org/10.1021/acsomega.3c02783
ACS Omega 2023, 8, 29388−29400

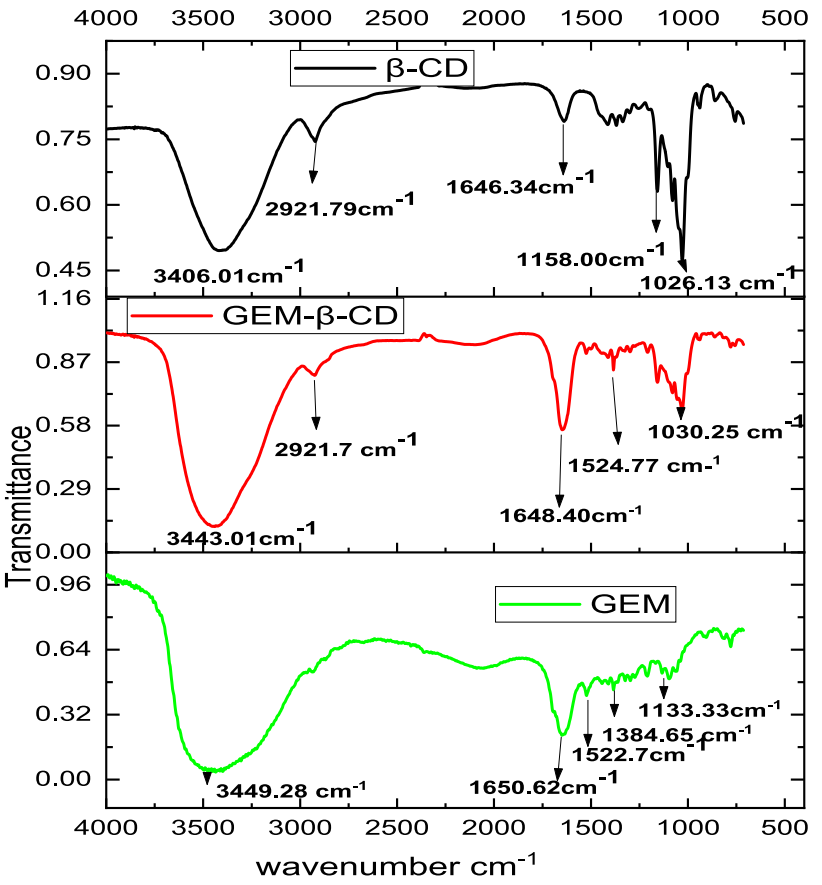

Figure 2. FT-IR spectra of the solid GEM-*β*-CD inclusion complex.

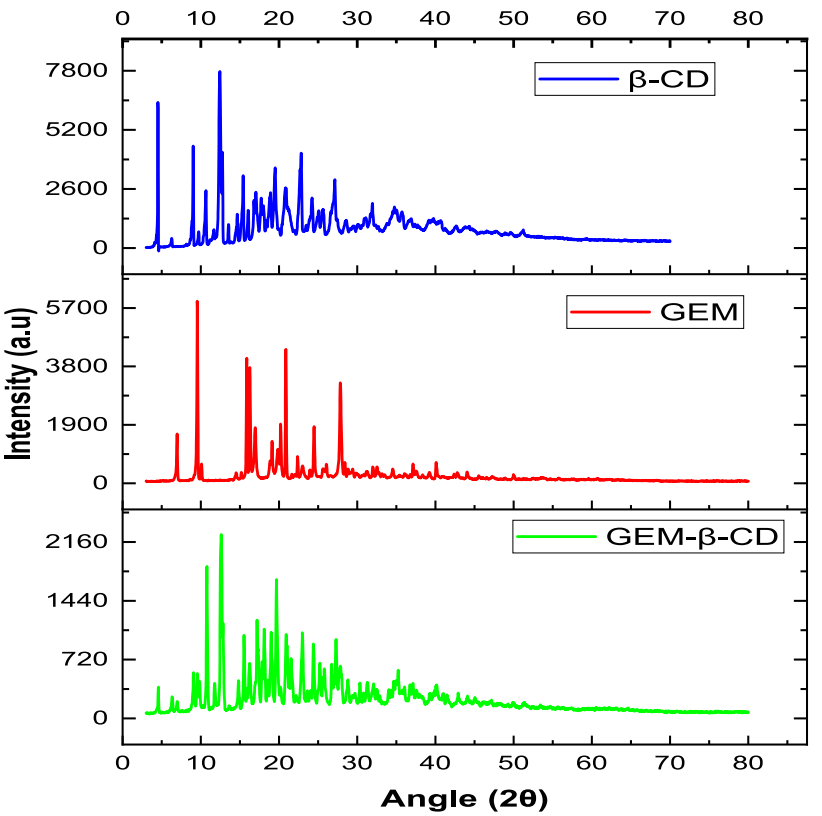

Figure 3. PXRD profiles of *β*-CD, GEM, and GEM-*β*-CD IC.

https://doi.org/10.1021/acsomega.3c02783
ACS Omega 2023, 8, 29388−29400

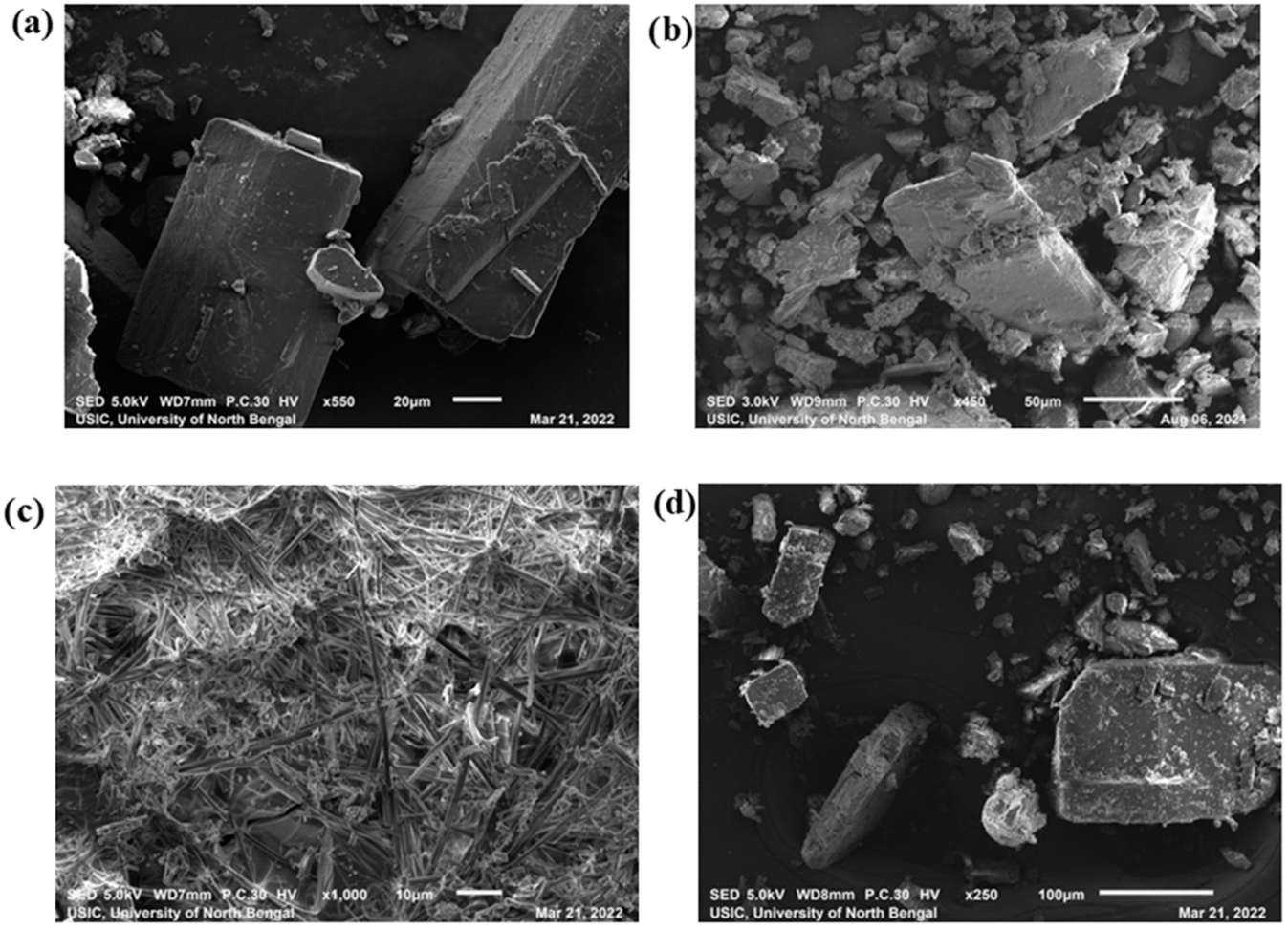

Figure 4. SEM images of (a) GEM, (b) β-CD, (c) GEM-β-CD complex (IC), and (d) physical mixture.

corresponding vibrational frequencies are outlined in Table S4. A sharp peak at 3443.10 cm^{-1} is observed in IC (GEM-β-CD), whereas a broad peak was recorded for both β-CD (3406.01 cm^{-1} corresponding to −OH stretching frequency) and GEM (3449.28 cm^{-1} corresponding to −OH and $-NH_2$ stretching frequency). The complete change in the nature of the peak may be attributed to the involvement of −OH bonds of both the drug and the host in interaction during complex formation. Again, the presence of a sharp peak in IC clearly indicates that the free $-NH_2$ bond is not involved in interaction with the host, thus supporting the findings of ^{1}H-NMR that the encapsulation happened through the five-membered ring, keeping the six-membered ring bearing the $-NH_2$ of GEM relatively free. This finding was further supported by the complete disappearance of the −OH bending frequency of both GEM (observed at 1133.33 cm^{-1}) and β-CD (observed at 1646.34 cm^{-1}) in IC. The C═O stretching frequency of the >CO moiety in GEM observed at 1650.62 cm^{-1} is shifted to 1648.40 cm^{-1} in IC. The slight change in $-NH_2$ bending frequency from 1522.70 cm^{-1} in GEM to 1524.77 cm^{-1} in IC also confirms that the -NH_2 bond in the six-membered ring is free and is not involved in the interaction with the host during encapsulation. This further indicates the possible insertion of GEM through five-membered rings. This is also supported by the appearance of C−N vibrations at the same position (1384.65 cm^{-1}) in both GEM and IC. The C−H and C−C−O stretching frequencies in β-CD previously observed at 2921.79 and 1026.13 cm^{-1} are found to be shifted to 2921.7 and 1030.25 cm^{-1}, respectively, in IC. The skeletal vibration arising due to the α-1,4-linkage at 951.95 cm^{-1} in β-CD is shifted to 939.52 cm^{-1} in the inclusion complex, which is mostly because of the introduction of GEM into the β-CD cavity. All of the above findings related to the intensities and shifts in the IR spectra convincingly present proof in support of inclusion complex formation and are in good agreement with the ^{1}H-NMR observations.

3.6. Powder XRD Analysis. The inclusion complex formation of GEM was further analyzed by the powder XRD technique.[52] A diagram consisting of the XRD patterns of β-CD, GEM, and the GEM-β-CD complex (IC) is shown in Figure 3. The crystalline diffractogram of β-CD exhibits sharp peaks at 4.52°, 9.02°, 10.47°, 19.50°, 20.82°, 22.83°, 24.21°, 25.62°, 27.13°, 31.10°, 31.93°, and 35.72°. The drug GEM also shows a well-defined sharp peak at 6.96, 9.55, 15.89, 16.27,16.95, 18.87, 19.11, 19.87, 20.20, 22.37°, 23.95°, 24.48°, 26.06°, 27.84°, 28.42°, 31.99°, 32.53°, 34.53°, 37.13°, 40.08°, 42.79°, 44.05°, and 49.98°, showing the presence of GEM in a crystalline state. Again, the XRD diffractogram of the GEM-β-CD complex presents a broad profile with changed 2θ value and decreased intensity of peaks. This is probably because the GEM got encapsulated inside the pocket of β-CD, resulting in a change in the vicinity of GEM and β-CD. Many characteristic peaks (15.87°, 19.11°, 23.95°, 32.53°, 34.53°, 37.13°, 40.79°, 44.05°, and 49.98°) present in the diffractogram of GEM have disappeared in the GEM-β-CD complex (IC). This observation

https://doi.org/10.1021/acsomega.3c02783
ACS Omega 2023, 8, 29388−29400

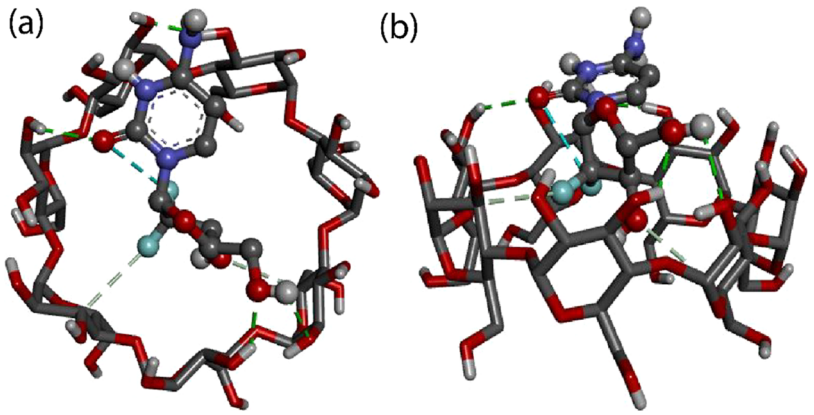

Figure 5. Geometry optimization of the molecules: (a) top and (b) side views of GEM-β-CD.

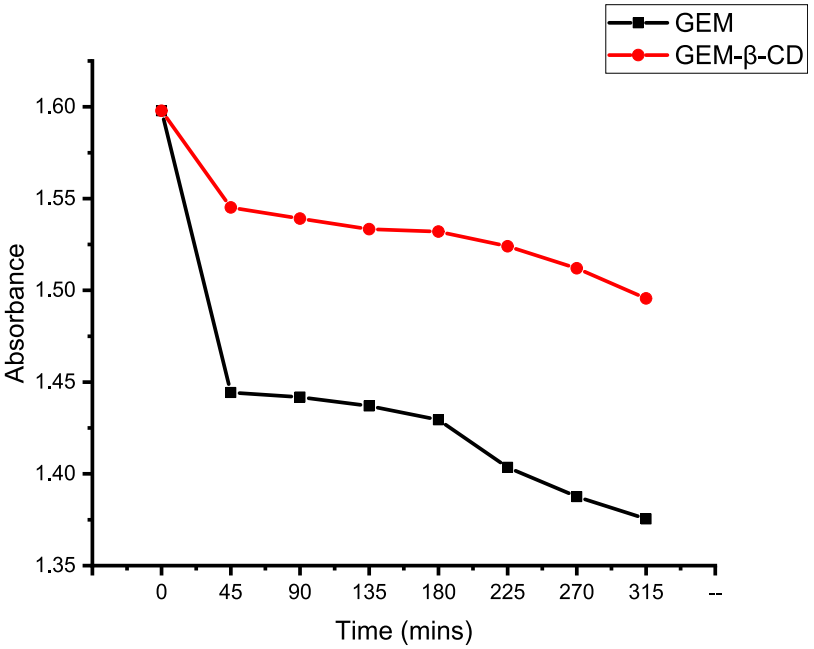

Figure 6. Comparative study of the photostabilities of GEM and IC (GEM-β-CD).

clearly indicates the change in the structure of GEM, thereby suggesting the formation of the inclusion complex. New diffraction peaks at $2\theta \simeq 12.60°$, 12.83°, 17.19°, 17.84°, and 18.10° have appeared in the powder XRD spectrum of GEM-β-CD. Further, the appearance of broader diffraction peaks with less intensity suggests that a new GEM-β-CD inclusion complex is formed and has attained a new crystalline structure.

3.7. SEM Analysis. The SEM study on host-guest chemistry is complementary evidence in support of inclusion complex formation.[50] This method provides a qualitative analysis on the morphology of the synthesized inclusion complex. This technique delivers an additional proof in support of inclusion complex formation by investigating the surface morphology of the host (β-CD), guest (GEM), GEM-β-CD IC, and the physical mixture of GEM and β-CD.[53] Figure 4 shows the SEM microphotographs of GEM, β-CD, IC, and the physical mixture of GEM and β-CD. Figure 4a shows a rod-like crystal structure of GEM, while the host β-CD (Figure 4b) shows crystalline irregular cubic particles having large features. The IC in Figure 4c shows long cylindrical rod-like dimensions linked together to form a cage type of structure, whereas the physical mixture (Figure 4d) shows distribution of particles of β-CD on the GEM surface, i.e., the original surface nature of both GEM and β-CD was present in the physical mixture, but in IC a new morphology was observed. Such marked improvement was observed in the surface morphology after the formation of the complex. Hence, the above results also reaffirm the encapsulation of GEM into the β-CD cavity to the form the solid GEM-β-CD inclusion complex.

3.8. Molecular Docking Evaluation. The molecular docking study is used to predict the orientation of the guest within the host cavity.[54] The docking is carried out between GEM and β-CD by employing PyRx software. The chief docked configuration of the GEM-β-CD complex is represented in Figure 5 (a, side view; b, top view). The minimum negative binding energy (ΔG) value for the best stable docked configuration of the GEM-β-CD complex is obtained as −5.40 kcal/mol, which is found to be very close to that for GEM-β-CD ($\simeq$ −5.84973 kcal/mol) obtained using UV−visible spectroscopic studies. This finding clearly suggests that the binding energy derived from docking correlates well with the data received from UV−visible absorption study. The docked

https://doi.org/10.1021/acsomega.3c02783
ACS Omega 2023, 8, 29388−29400

conformation of the GEM-β-CD complex shows that the *deoxycytidine moiety* of GEM was included into the hydrophobic pocket of β-CD near the wider rim, while the *pyrimidine* moiety of GEM was found to be present outside the wider rim of the β-CD cavity. Further, the docked conformation is stabilized by the strong hydrogen bonding of the fluoride atoms of GEM with the H-3 protons of β-CD. These interactions of GEM with β-CD observed in the docking study analysis show good correlation with those of ^{1}H-NMR and FT-IR analysis.

3.9. Photostability Analysis of the Inclusion Complex. The above observations clearly indicate that a stable inclusion complex with 1:1 stoichiometry of GEM with β-CD has been formed. Therefore, it is very important to investigate its stability with regard to UV−visible light. The improvement in photostability of GEM through complexation would assuredly enhance its use in vast therapeutic and optical fields. UV−vis spectrophotometric measurements were used to study the photostability of the drug and that of the complex in water solutions. GEM and IC were irradiated in sunlight continuously for more than 5 h and at a regular interval of 45 min their absorption spectra were taken. For this purpose, 100 μM solutions of GEM (6.5 mg in 100 mL) and IC GEM-β-CD (6.18 mg in 50 mL) were prepared. The solutions were left for 1 h with continuous stirring to attain equilibrium. Thereafter, a series of absorption spectra were recorded for both GEM and IC solutions before irradiation and subsequently after (at 45 min regular interval) irradiation with the sunlight by taking a 3 mL solution each time. A regular decrease in the absorbance (at 268 nm) for all solutions was observed upon irradiation. Evaluation of spectral data revealed that the photostability of GEM was increased manifold by complexation with β-CD. To measure the stability, photodegradation efficiency was evaluated using following eq 3

$$\% \text{ of degradation} = [(A_0 - A_T)/A_0] \times 100 \quad (3)$$

where A_0 is the initial absorbance and A_T is the absorbance of the sample irradiated at time interval T in minutes.

A comparative study of the photostability of GEM with IC is shown in Figure 6. A critical analysis of the figures displays that the photostability of GEM has been improved upon complexation and IC is more stable to UV−visible light when exposed to sunlight. The degradation percentage for GEM and that of IC are found to be 13.00 and 4.00%, respectively, as calculated using eq 3. Hence, nearly 3.5 times increase in the stability has been achieved through IC formation. This finding is indeed an absolute indication of the greater photostability of IC over GEM. The incredible boost in stability of GEM upon encapsulation with CDs may be assigned to the shielding laid by the β-CD cavity owing to the encapsulation, subsequently reducing the degradation due to UV-light effects when compared with the free drug.[55,56]

3.10. In Vitro Studies of Biological Activity. *3.10.1. In Vitro Antiproliferative Assay.* GEM and GEM-β-CD IC were assayed for their potential antiproliferative activity against the normal human cell line using MTT assay. The effect of GEM and inclusion complex IC (GEM-β-CD) on human cells was highly significant and both the compounds exhibited pronounced antiproliferative activity in a dose-dependent manner (Figure S4). The strongest antiproliferative activity was demonstrated by GEM, and in comparison, a slightly decreased activity was observed for IC (GEM-β-CD). This *in vitro* result suggests that, upon formation of the inclusion complex of GEM, IC (GEM-β-CD) may decrease the cytotoxicity in normal human cells at all tested concentrations. Due to this precise decrease in toxicity against normal human cells exhibited by IC (GEM-β-CD), it has been identified as a promising drug candidate suitable for clinical use. Further studies are therefore needed to evaluate the contributing role of the inclusion complex IC (GEM-β-CD) in exhibiting reduced cytotoxicity ($p < 0.05$) against normal human cells relative to the parent compound GEM. The results of the present study will have potential direct impacts on human health and clinical applications as reduced cytotoxicity complements to reduced side effects. Recent research on the inclusion complex brings evidence that the most plausible mechanisms of action involve the sustained release of GEM from the cavity of β-CD, thereby decreasing the magnitude of toxicity of GEM through encapsulation with β-CD.[57] In the present study, it was found that the IC (GEM-β-CD) (IC_{50} = 11.35 μM) complex exhibited slight increase in activity, manifesting a less cytotoxic character than pure GEM (IC_{50} = 11.52 μM) toward the human cell line, suggesting that inclusion has diminished the side effects of GEM to a certain level. The concrete mechanism of the action of toxicity against the healthy test cell line is not established in the present study, but previous studies suggest that such reduction is due to the drug complexation. Further, the interaction study of IC and GEM with CT-DNA in this work suggests improved interaction after complexation compared with GEM, indicating that complexation of GEM in β-CD is one of the ways to decrease toxicity. The larger binding constant for DNA-(GEM-β-CD) (8.1575 × 1010) as compared to DNA-(GEM) (5.954579 ×108) strongly supports the drug-DNA binding mode that is observed in the studied compound GEM-β-CD.

3.10.2. In Vitro Antibacterial Activity Studies. Prolonged use of chemotherapy drugs may lead patients to a risk of infection by weakening the immune systems. Repeated hospitalization during chemotherapy treatment may induce bacterial infection, thus declining the survival rate among patients. Many antimicrobial and antibacterial therapies have been developed in the past few decades. But, due to the antibacterial resistance slowly developed by these species, the currently available antibiotics has limited application.[58−63] Under such scenario, it is very urgent to design and develop an effective antibacterial agent to be used in such therapies. Hence, it is of utmost importance for an anticancer drug to possess antibacterial effect such that it reduces the side effect of cancer treatment. The results obtained from the disc diffusion assay showed that there has been a significant increasing effect of GEM and the GEM-β-CD complex (GEM-β-CD) on bacterial growth inhibition (Tables S5 and S6). The drugs with increasing concentration from 3.9 to 1000 μM exhibited a broad-spectrum activity against all of the tested organisms. *Staphylococcus aureus*, a Gram-positive bacterium, showed the highest sensitivity in the disc diffusion test when treated with 1000 μM of GEM and the GEM-β-CD complex, and the inhibition zones recorded were 38.66 and 39.66 mm, respectively. Likewise, the recorded inhibition zones of *Klebsiella pneumoniae*, a Gram-negative bacterium, when treated with 1000 μM of GEM and the GEM-β-CD complex resulted in an inhibition of 32.33 and 34.33 mm, respectively. The lowest zone of inhibition (ZOI) was recorded in GEM at a concentration of 3.9 μM with an inhibition zone of 16 mm against *S. aureus*. Comparatively, the GEM-β-CD complex was found to remain highly effective even at the lowest tested concentration of 3.9 μM with inhibition zones of 7.33, 8.66, and 8.66 mm against *S. aureus*, *B. cereus*, and *S. pneumoniae*, respectively. At present, however, there has been no specific

https://doi.org/10.1021/acsomega.3c02783
ACS Omega 2023, 8, 29388−29400

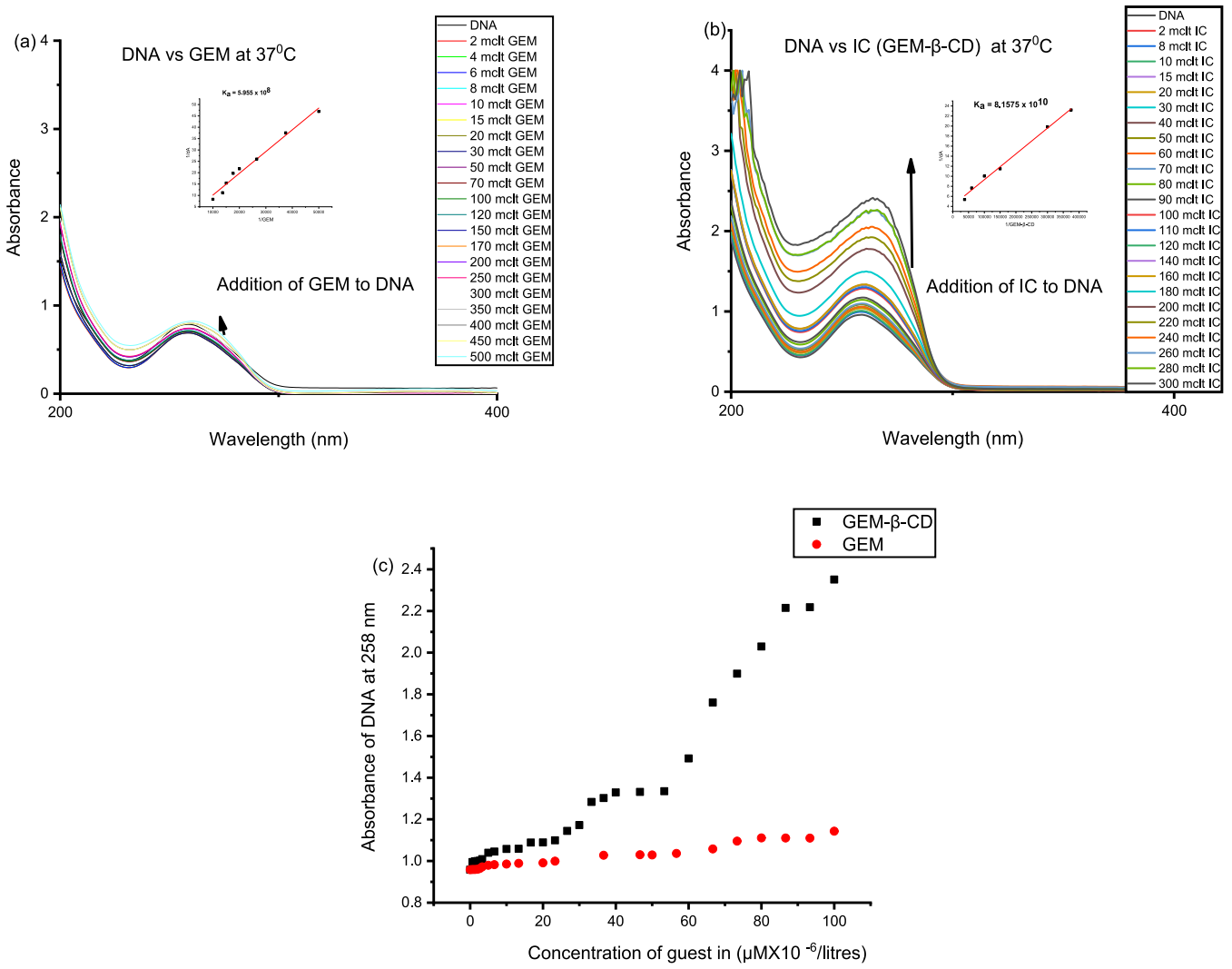

Figure 7. UV−visible spectra of CT-DNA at different concentrations of (a) GEM, (b) IC (GEM-β-CD), and (c) comparison of CT-DNA interaction with GEM and IC (GEM-β-CD).

cutoff value reported as a gold standard for analyzing the antibacterial activity of GEM and the GEM-β-CD complex (GEM-β-CD). A 1/2 dilution within the test cutoff concentration value of 1000 μM exhibited active antibacterial activity even at 1/16 dilution in case of the GEM-β-CD complex against *S. aureus*, *B. cereus*, and *S. pneumoniae*, and this prominent biological activity of the synthesized drug warrants further investigation as a substitute for novel anti-infective agents. Thus, it is evident from the present study that GEM and the GEM-β-CD complex showed comparable antimicrobial activities with chloramphenicol as a reference standard (Tables S5 and S6) (Figures S5 and S6). With these inhibitory properties, it is rational for a researcher to develop newer antibacterial drugs through conversion of the parent drug in use to replenish the depleted pipeline of the antibacterial drugs with a new structural property. Around the globe, antimicrobial resistance relegates many miracle drugs currently in use to the dust heap. Therefore, biomedical science needs other inexpensive designer drugs to take their place, and the properties demonstrated by the GEM-β-CD complex in the present study cannot be ruled out.

3.11. CT-DNA Interaction Study with Gemcitabine and the Prepared IC. The intensive laboratory research on drug-DNA interactions has generated much experimental data, which could enhance our understanding of drug-DNA interactions at the molecular level. Such interaction studies have vast applications in clinical research and have been in prime focus to design new efficient drug delivery systems.[64−66] Studies on drugs complexed with cyclodextrins (CDs) revealed that CDs play a pivotal role in drug delivery, which can enhance the biocompatibility of various drug molecules in transmembrane transport.[63] The present investigation clearly revealed that GEM and the inclusion complex IC GEM-β-CD had significant *in vitro* biological activity. One of the key mechanisms for the efficient CT-DNA interaction relates to the lipophilic nature of GEM, which allows it to overcome membrane barriers and thereby facilitates its entry inside the cell with help of nucleoside membrane transporters. The studies by other workers have reported that GEM undergoes phosphorylation and eventually interferes with the replication machinery by competing with the cytidine derivatives. GEM triphosphate at higher concentrations is believed to hinder the function of cytidine triphosphate (CTP) synthetase and cytidine monophosphate (CMP) deaminase, which results in low CTP concentrations.[67] It is well established that GEM exerts its biological activity involving two mechanistic pathways.[68] The first mechanism involves the integration of GEM into DNA during the repair process, in

https://doi.org/10.1021/acsomega.3c02783
ACS Omega 2023, 8, 29388−29400

which the base excision enzymes fail to remove the GEM triphosphate, thereby blocking DNA synthesis.[67,69] The second mechanism of GEM triphosphate involves the inhibition of an enzyme namely ribonucleotide reductase that is responsible for nascent DNA strand synthesis.[67,69] To verify the CT-DNA interactions with GEM and GEM-β-CD, a fixed concentration of calf thymus-DNA (0.11 μg/mL) was prepared in a fresh solution of Tris-HCl buffer (0.01 M, pH 7.0), to which different concentrations of GEM and GEM-β-CD were added in a reaction tube. We evaluated the absorption spectra of each reaction mixture incubated at 37 °C after 30 min (Figure 7). A double reciprocal graph was plotted using Benesi-Hildebrand equation (eq 4) and intrinsic binding constants (K_a) were calculated (Table 1). A hyperchromic shift was observed with

Table 1. Binding Constants of CT-DNA Interaction with GEM and IC (GEM-β-CD)

binding constant (M^{-1})	GEM	IC (GEM-β-CD)
K_a	5.95×10^8	8.16×10^{10}

the continuous increase of concentrations of GEM and GEM-β-CD to DNA solution, which was due to the conformational changes caused by DNA-GEM and DNA-(GEM-β-CD) interactions. The results in this study distinctly show an enhancement in molar absorptivity (hyperchromism), which is due to the structural reorganization of CT-DNA as discussed above. Interactions of DNA with GEM and GEM-β-CD at the level of 0.11 μg/mL and its subsequent hyperchromic shift clearly show that the formation of the inclusion complex may improve the biological property of GEM (Figure 7). The enhancement in absorptivity of mixtures might partly be assigned to the disturbance of forces binding the double helical structure, thereby disrupting the double helix, which finally leads to the generation of single strands. The binding constant of GEM with CT-DNA has been found to increase many folds after complexation (Table 1). In this study, IC (GEM-β-CD) exhibited reduced toxicity toward healthy human cells as compared to free GEM. Remarkably, the higher binding constant clearly suggests the interaction to be groove binding. Thus, the high binding constant in IC (GEM-β-CD) seems to suggest that owing to the inclusion complex formation, the interaction of GEM with CT-DNA has improved as compared to that between free GEM and CT-DNA. In the present study, we found that the interaction of DNA with both GEM and GEM-β-CD is groove binding, as evident from the binding constant value (Table 1). Generally, they have a crescent shape complementing the shape of the groove,[70] which makes binding much easier by stimulating van der Waals interactions. Since GEM has furan moiety (Figure S8) connected through bonds having torsional freedom, it can form hydrogen bonds with bases, especially to those with sequences rich in adenine/thymine. In such compounds, the drug fits comfortably into the groove and replaces the hydration layer. In the complex structure, the helical twist is altered from the uncomplexed alternating DNA. One of the bases of DNA rotates to facilitate hydrogen bonding with the drug, or the bonding is supported through a water molecule in between the drug and the DNA, where water is serving as a balancing force. Additionally, the normal Watson/Crick geometry of the DNA helix structure remarkably suffers major perturbation through van der Waals forces. Apart from the changes in structure of DNA, these interactions also initiate the changes in the conformation of the drug due to groove binding. Thus, the increase in interaction and binding constant may be attributed to the sustained release of the drug after inclusion complex formation. Inclusion complex formation may increase groove binding by stabilizing the drug-DNA interaction with proper orientation (Figure 5). Thus, preclinical studies on DNA interaction activity using various *in vivo* models will be needed to confirm the mechanism of enhancement of DNA interaction through inclusion complex formation for therapeutic application.

$$\frac{1}{\Delta A} = \frac{1}{\Delta\varepsilon[\mathrm{DNA}]K_a}\frac{1}{[\mathrm{GEM}]} + \frac{1}{\Delta\varepsilon[\mathrm{DNA}]} \quad (4)$$

where $\Delta\varepsilon$ is the difference in molar absorption coefficient of DNA in the presence and absence of GEM and ICs. From the K_a values it is evident that the interaction follows the following order

$$\mathrm{DNA} - (\mathrm{GEM} - \beta - \mathrm{CD}) > \mathrm{DNA} - \mathrm{GEM}$$

4. CONCLUSIONS

Herein, we have reported the successful formation of the inclusion complex of gemcitabine with β-cyclodextrin both in solid and in solution phase. The preparation of the inclusion complex has successfully reduced the toxicity of GEM by maintaining the sustained release of the drug. The results of ^{1}H-NMR, ESI-MS, FT-IR, SEM, PXRD, and UV−vis spectroscopic analysis clearly indicate that gemcitabine was efficiently incorporated in the complexation with β-cyclodextrin. The ESI-MS experiment and Job's plot confirmed the 1:1 stoichiometry of the IC complex. Determination of the binding constant value ($K_a = 19.4 \times 10^3\ M^{-1}$) for IC (GEM-$\beta$-CD) and negative Gibb's free energy change (ΔG) confirmed the thermodynamic spontaneity of the binding process. ^{1}H-NMR, FT-IR, and computational studies revealed the formation of a stable inclusion complex of GEM with β-CD, where the GEM is inserted into the cavity of β-CD. SEM and PXRD analysis suggested that the synthesized complex IC (GEM-β-CD) has crystalline morphology, which is distinctly different from that of GEM and β-CD. Based on the photodegradation profiles of IC (GEM-β-CD), our percentage of photodegradation of GEM has been improved significantly from 13% in free GEM to 4% IC (GEM-β-CD), which in turn clearly indicates the higher stability of GEM toward ultraviolet light after the inclusion phenomena. Consequently, this observation not only supports the possible application of gemcitabine in optical field but also proves that it may show increased efficacy when used as a chemotherapy drug. *In vitro* antibacterial test showed that the activity was improved, as displayed by GEM after its complexation with β-CD. However, IC (GEM-β-CD) showed similar antibacterial activity against some pathogens as that shown by GEM. However, IC (GEM-β-CD) showed comparable antibacterial activity against bacterial pathogens to that shown by GEM. Apparently, as shown by antibacterial assay, IC (GEM-β-CD) could be a promising drug alternative for bacterial pathogens that have acquired resistance against GEM. Further, it has been established that the participation of gemcitabine in complexation with β-CD effectively inhibited bacterial growth in comparison to its free form. To define the potency of the GEM and inclusion complexes, the IC_{50} was determined. The IC_{50} value represent the concentration resulting in 50% cell growth inhibition of the cell line tested. In the present study, it was recorded that the IC (GEM-β-CD) (IC_{50} = 11.35 μM)

https://doi.org/10.1021/acsomega.3c02783
ACS Omega 2023, 8, 29388−29400

complex exhibited slightly increased activity, manifesting a less cytotoxic character than pure GEM (IC_{50} = 11.52 μM) toward the human cell line and suggesting that inclusion has sufficiently decreased the side effect of GEM to a certain level. The exact mechanism of reduction in toxicity against the healthy test cell line is not fully established in the present study, but previous studies imply that such reduction is facilitated by drug complexation. Importantly, the interaction study of IC and GEM with CT-DNA in this work further revealed improved interaction after complexation compared with GEM, suggesting that complexation of GEM in β-CD is essential. The larger binding constant for DNA-(GEM-β-CD) (8.1575×10^{10}) as compared to DNA-(GEM) (5.954579×10^{8}) strongly favors the drug-DNA binding mode that is observed in the compound GEM-β-CD studied herein.

To conclude, the formation of the inclusion complex of GEM with β-CD has opened a new paradigm for novel formulation of GEM in drug delivery and optical application, thus expanding or preserving the spectrum of medical application of GEM in pharmaceutical industries and biomedical sciences with decreased toxicity.

■ ASSOCIATED CONTENT

Supporting Information

The Supporting Information is available free of charge at https://pubs.acs.org/doi/10.1021/acsomega.3c02783.

Different data for Job plots ^{1}H-NMR, FT-IR, data for photostability plot, CT-DNA interaction plot (PDF)

Different figures such as 1H-NMR, ESI-MS are included in supporting information (PDF)

■ AUTHOR INFORMATION

Corresponding Author

Mahendra Nath Roy − *Department of Chemistry, University of North Bengal, Darjeeling 734013, India;* orcid.org/0000-0002-7380-5526; Email: mahendraroy2002@yahoo.co.in

Authors

Antara Sharma − *Department of Chemistry, University of North Bengal, Darjeeling 734013, India; Department of Chemistry, St. Joseph's College, Darjeeling 734104, India*

Pranish Bomzan − *Department of Chemistry, Gorubathan Government College, Kalimpong 735231, India*

Niloy Roy − *Department of Chemistry, University of North Bengal, Darjeeling 734013, India*

Vikas Kumar Dakua − *Department of Chemistry, Alipurduar University, Alipurduar 736122, India*

Kanak Roy − *Department of Chemistry, Alipurduar University, Alipurduar 736122, India*

Abhinath Barman − *Department of Physics, Alipurduar University, Alipurduar 736122, India*

Rabindra Dey − *Department of Chemistry, Cooch Behar College, Cooch Behar 736101, India*

Abhijit Chhetri − *Department of Microbiology, St. Joseph's College, Darjeeling 734104, India*

Rajani Dewan − *Department of Chemistry, St. Joseph's College, Darjeeling 734104, India*

Ankita Dutta − *Department of Biotechnology, University of North Bengal, Darjeeling 734013, India*

Anoop Kumar − *Department of Biotechnology, University of North Bengal, Darjeeling 734013, India*

Complete contact information is available at: https://pubs.acs.org/10.1021/acsomega.3c02783

Notes

The authors declare no competing financial interest.

■ ACKNOWLEDGMENTS

The authors are thankful to the Department of Chemistry and Department of Biotechnology, University of North Bengal, Darjeeling, WB for assistant instrumental support. The authors are also thankful to SAIF-COCHIN and SAIF-PANJAB UNIVERSITY for additional instrumental facility.

■ REFERENCES

(1) Wild, C. P.; Weiderpass, E.; Stewart, B. W. *World Cancer Report*; World Health Organization Press: Lyon, 2020.

(2) Boyle, P.; Lyon, B. L. *World Cancer Report*; World Health Organization Press: Geneva, 2008.

(3) Burris, H. A.; Moore, M. J.; Andersen, J.; Green, M. R.; Rothenberg, M. L.; Modiano, M. R.; Cripps, M. C.; Portenoy, R. K.; Storniolo; Tarassoff, A. M.; Nelson, P. R.; Dorr, F. A.; Stephens, C. D.; Von Hoff, D. D. Improvements in survival and clinical benefit with gemcitabine as first-line therapy for patients with advanced pancreas cancer: a randomized trial. *J. Clin. Oncol.* **1997**, *15*, 2403−2413.

(4) Devulapally, R.; Paulmurugan, R. Polymer nanoparticles for drug and small silencing RNA delivery to treat cancers of different phenotypes. *Wiley. Interdiscip. Rev.: Nanomed. Nanobiotechnol.* **2014**, *6*, 40−60.

(5) Shaaban, S.; Negm, A.; Ibrahim, E. E.; Elrazak, A. A. Chemotherapeutic agents for the treatment of hepatocellular carcinoma: efficacy and mode of action. *Oncol Rev.* **2014**, *8*, 246.

(6) (a) Hertel, L. W.; Boder, G. B.; Kroin, J. S.; Rinzel, S. M.; Poore, G. A.; Todd, G. C.; Grindey, G. B. Evaluation of the antitumor activity of gemcitabine (2′,2′-difluoro-2′-deoxycytidine). *Cancer Res.* **1990**, *50*, 4417−4422. (b) Braakhuis, B. J.; Ruiz van Haperen, V. W.; Welters, M. J.; Peters, G. J. Schedule-dependent therapeutic efficacy of the combination of gemcitabine and cisplatin in head and neck cancer xenografts. *Eur. J. Cancer* **1995**, *31*, 2335−2340. (c) Merriman, R. L.; Hertel, L. W.; Schultz, R. M.; Houghton, P. J.; Houghton, J. A.; Rutherford, P. G.; Tanzer, L. R.; Boder, G. B.; Grindey, G. B. Comparison of the antitumor activity of gemcitabine and ara-C in a panel of human breast, colon, lung and pancreatic xenograft models. *Invest. New Drugs* **1996**, *14*, 243−247. (d) Manegold, C. Gemcitabine (Gemzar) in non-small cell lung cancer. *Expert Rev. Anticancer Ther.* **2004**, *4*, 345−360. (e) Heinemann, V. Gemcitabine in metastatic breast cancer. *Expert Rev. Anticancer Ther.* **2005**, *5*, 429−443.

(7) Eckel, F.; Schneider, G.; Schmid, R. M. Pancreatic cancer: a review of recent advances. *Expert Opin. Invest. Drugs* **2006**, *15*, 1395−1410.

(8) Toschi, L.; Finocchiaro, G.; Bartolini, S.; Gioia, V.; Cappuzzo, F. Role of gemcitabine in cancer therapy. *Future Oncol.* **2005**, *1*, 7−17.

(9) Beumer, J. H.; Eiseman, J. L.; Parise, R. A.; Joseph, E.; Covey, J. M.; Egorin, M. J. Modulation of gemcitabine (2′, 2′-difluoro-2′-deoxycytidine) pharmacokinetics, metabolism, and bioavailability in mice by 3, 4, 5, 6-tetrahydrouridine. *Clin. Cancer Res.* **2008**, *14*, 3529−35.

(10) Gilbert, J. A.; Salavaggione, O. E.; Ji, Y.; Pelleymounter, L. L.; Eckloff, B. W.; Wieben, E. D.; Ames, M. M.; Weinshilboum, R. M. *Clin. Cancer Res.* **2006**, *12*, 1794−803.

(11) Heinemann, V.; Xu, Y. Z.; Chubb, S.; Sen, A.; Hertel, L. W.; Grindey, G. B.; Plunkett, W. Gemcitabine Pharmacogenomics: Cytidine Deaminase and Deoxycytidylate Deaminase Gene Resequencing and Functional Genomics. *Cancer Res.* **1992**, *52*, 533−539.

(12) Bergman, A. M.; Adema, A. D.; Balzarini, J.; Bruheim, S.; Fichtner, I.; Noordhuis, P.; Fodstad, O.; Myhren, F.; Sandvold, M. L.; Hendriks, H. R.; Peters, G. J. Antiproliferative activity, mechanism of action and oral antitumor activity of CP-4126, a fatty acid derivative of gemcitabine, in in vitro and in vivo tumor models. *Invest. New Drugs* **2011**, *29*, 456−466.

(13) Reddy, L. H.; Couvreur, P. Novel approaches to deliver gemcitabine to cancers. *Curr. Pharm. Des.* **2008**, *14*, 1124−1137.
(14) Pasut, G.; Canal, F.; Dalla Via, L.; Arpicco, S.; Veronese, F. M.; Schiavon, O. Antitumoral activity of PEG−gemcitabine prodrugs targeted by folic acid. *J. Controlled Release* **2008**, *127*, 239−248.
(15) Conroy, T.; Desseigne, F.; Ychou, M.; Bouché, O.; Guimbaud, R.; Bécouarn, Y.; Adenis, A.; Raoul, J. L.; Gourgou-Bourgade, S.; de la Fouchardière, C.; Bennouna, J. B.; Michel; Bachet, B.; Khemissa-Akouz, F.; Péré-Vergé, D.; Delbaldo, C.; Assenat, E.; Chauffert, B.; Montoto-Grillot, P. C.; Ducreux, M. FOLFIRINOX versus gemcitabine for metastatic pancreatic cancer. *N. Engl. J. Med.* **2011**, *364*, 1817−25.
(16) Conroy, T.; Hammel, P.; Hebbar, M.; Ben Abdelghani, M.; Wei, A. C.; Raoul, J. L.; Choné, L.; Francois, E.; Artru, P.; Biagi, J. J.; Lecomte, T.; Assenat, E.; Faroux, R.; Ychou, M.; Volet, J.; Sauvanet, A.; Breysacher, G.; Di Fiore, F.; Cripps, C.; Kavan, P.; Texereau, P.; Bouhier-Leporrier, K.; Khemissa-Akouz, F.; Legoux, J. L.; Juzyna, B.; Gourgou, S.; O'Callaghan, C. J.; Jouffroy-Zeller, C.; Rat, P.; Malka, D.; Castan, F.; Bachet, J. B. FOLFIRINOX or gemcitabine as adjuvant therapy for pancreatic cancer. *N. Engl. J. Med.* **2018**, *379*, 2395−2406.
(17) Cai, H.; Wang, R.; Guo, X.; Song, M.; Yan, F.; Ji, B.; Liu, Y. Combining gemcitabine-loaded macrophage-like nanoparticles and erlotinib for pancreatic cancer therapy. *Mol. Pharmaceutics* **2021**, *18*, 2495−2506.
(18) Emamzadeh, M.; Emamzadeh, M.; Pasparakis, G. Dual controlled delivery of gemcitabine and cisplatin using polymer-modified thermosensitive liposomes for pancreatic cancer. *ACS Appl. Bio Mater.* **2019**, *2*, 1298−1309.
(19) Karampelas, T.; Skavatsou, E.; Argyros, O.; Fokas, D.; Tamvakopoulos, C. Gemcitabine based peptide conjugate with improved metabolic properties and dual mode of efficacy. *Mol. Pharmaceutics* **2017**, *14*, 674−685.
(20) Kulhari, H.; Pooja, D.; Kota, R.; Telukutla, S. R.; Tabor, R. F.; Shukla, R.; Adams, D. J.; Sistla, R.; Bansal, V. Cyclic RGDfK peptide functionalized polymeric nanocarriers for targeting gemcitabine to ovarian cancer cells. *Mol. Pharmaceutics* **2016**, *13*, 1491−1500.
(21) Kamisawa, T.; Wood, L. D.; Itoi, T.; Takaori, K. Pancreatic cancer. *Lancet* **2016**, *388*, 73−85.
(22) Mollberg, N.; Rahbari, N. N.; Koch, M.; Hartwig, W.; Hoeger, Y.; Büchler, M. W.; Weitz, J. Arterial resection during pancreatectomy for pancreatic cancer: a systematic review and meta-analysis. *Ann. Surg.* **2011**, *254*, 882−93.
(23) Vincent, A.; Herman, J.; Schulick, R.; Hruban, R. H.; Goggins, M. Pancreatic cancer. *Lancet* **2011**, *378*, 607−20.
(24) Zeng, S.; Pöttler, M.; Lan, B.; Grützmann, R.; Pilarsky, C.; Yang, H. Chemoresistance in pancreatic cancer. *Int. J. Mol. Sci.* **2019**, *20*, 4504.
(25) Amrani, M. E.; Corfiotti, F.; Corvaisier, M.; Vasseur, R.; Fulbert, M.; Skrzypczyk, C.; Deshorgues, A. C.; Gnemmi, V.; Tulasne, D.; Lahdaoui, F.; Vincent, A.; Pruvot, F. R.; Seuningen, I. V.; Huet, G.; Truant, S. Therapeutic resistance of pancreatic cancer: Roadmap to its reversal. *Mol. Carcinog.* **2019**, *58*, 1985−1997.
(26) Chen, Z.; Zheng, Y.; Shi, Y.; Cui, Z. Overcoming tumor cell chemoresistance using nanoparticles: lysosomes are beneficial for (stearoyl) gemcitabine-incorporated solid lipid nanoparticles. *Int. J. Nanomed.* **2018**, *13*, 319−336.
(27) Wei, L.; Wen, J. Y.; Chen, J.; Ma, X. K.; Wu, D. H.; Chen, Z. H.; Huang, J. L. Oncogenic ADAM28 induces gemcitabine resistance and predicts a poor prognosis in pancreatic cancer. *World J. Gastroenterol.* **2019**, *25*, 5590−5603.
(28) Moore, M. J.; Goldstein, D.; Hamm, J.; Figer, A.; Hecht, J. R.; Gallinger, S.; Au, H. J.; Murawa, P.; Walde, D.; Wolff, R.; Campos, D.; Lim; Ding, R. K.; Clark, G.; Voskoglou-Nomikos, T.; Ptasynski, M.; Parulekar, W. Erlotinib Plus Gemcitabine Compared With Gemcitabine Alone in Patients With Advanced Pancreatic Cancer: A Phase III Trial of the National Cancer Institute of Canada Clinical Trials Group. *J. Clin. Oncol.* **2007**, *25*, 1960−6.
(29) Patil, P. S.; Kadam, D. V.; Marapur, S. C.; Kamalapur, M. V. Inclusion Complex System; A Novel Technique to Improve the Solubility and Bioavailability of Poorly Soluble Drugs: A Review. *Int. J. Pharm. Sci. Rev. Res.* **2010**, *2*, No. 006.
(30) Carneiro, S. B.; Duarte, F. Í. C.; Heimfarth, L.; Quintans, J. de S. S.; Quintans-Júnior, L. J.; da Veiga Júnior, V. F.; Neves de Lima, Á. A. Cyclodextrin−drug inclusion complexes: In vivo and in vitro approaches. *Int. J. Mol. Sci.* **2019**, *20*, No. 642.
(31) Kfoury, M.; Landy, D.; Fourmentin, S. Characterization of cyclodextrin/volatile inclusion complexes: a review. *Molecules* **2018**, *23*, No. 1204.
(32) Tian, B.; Xiao; Hei, D. T.; Ping, R.; Hua, S.; Liu, J. The application and prospects of cyclodextrin inclusion complexes and polymers in the food industry: A review. *Polym. Int.* **2020**, *69*, 597−603.
(33) dos Santos Lima, B.; Shanmugam, S.; de Souza Siqueira Quintans, J.; Quintans-Junior, L. J.; de Souza Arau′jo, A. A. Inclusion complex with cyclodextrins enhances the bioavailability of flavonoid compounds: A systematic review. *Phytochem. Rev.* **2019**, *18*, 1337−1359.
(34) Bhattacharya, P.; Sahoo, D.; Chakravorti, S. Photophysics and structure of inclusion complex of 4, 4-diaminodiphenyl sulfone with cyclodextrin nanocavities. *Ind. Eng. Chem. Res.* **2011**, *50*, 7815−7823.
(35) Roy, N.; Ghosh, B.; Roy, D.; Bhaumik, B.; Roy, M. N. Exploring the Inclusion Complex of a Drug (Umbelliferone) with α-Cyclodextrin Optimized by Molecular Docking and Increasing Bioavailability with Minimizing the Doses in Human Body. *ACS Omega* **2020**, *5*, 30243−30251.
(36) Rajbanshi, B.; Saha, S.; Das, K.; Barman, B. K.; Sengupta, S.; Bhattacharjee, A.; Roy, M. N. Study to Probe Subsistence of Host-Guest Inclusion Complexes of α and β-Cyclodextrins with Biologically Potent Drugs for Safety Regulatory Dischargement. *Sci. Rep.* **2018**, *8*, No. 13031.
(37) Caso, J. V.; Russo, L.; Palmieri, M.; Malgieri, G.; Galdiero, S.; Falanga, A.; Isernia, C.; Iacovino, R. Alpha- and Beta-Cyclodextrin Inclusion Complexes with 5-Fluorouracil: Characterization and Cytotoxic Activity Evaluation. *Amino Acids* **2015**, *47*, 2215−2227.
(38) Ramos, A. I.; Braga, T. M.; Silva, P.; Fernandes, J. A.; Ribeiro-Claro, P. M.; Lopes, D.F.S.; Paz, F. A. A.; Braga, S. S. Chloramphenicol·cyclodextrin inclusion compounds: co-dissolution and mechanochemical preparations and antibacterial action. *Cryst. Eng. Comm* **2013**, *15*, 2822−2834.
(39) Frisch, M. J.; Trucks G, W.; Schlegel, H. B.; Scuseria, G. E.; Robb, M. A.; Cheeseman J, R.; Scalmani, G.; Barone, V.; Petersson, G. A.; Nakatsuji, H.; Caricato, X.; Li, M.; Marenich, A.; Bloino, J.; Janesko, B. G.; Gomperts, R.; Mennucci, B.; Hratchian, H. P.; Ortiz, J. V.; Izmaylov, A. F.; Sonnenberg, J. L.; Williams-Young, D.; Ding, F.; Lipparini, F.; Egidi, F.; Goings, J.; Peng, B.; Petrone, A.; Henderson, T.; Ranasinghe, D.; Zakrzewski, V. G.; Gao, J.; Rega, N.; Zheng, G.; W Liang, M.; Hada, M.; Ehara, K.; Toyota, R.; Fukuda, J.; Hasegawa, M.; Ishida, T.; Nakajima, Y.; Honda; Kitao, O.; Nakai, H.; Vreven, T.; Throssell, K.; Montgomery, J. A.; Peralta, J. E., Jr.; Ogliaro, F.; Bearpark, M.; Heyd, J. J.; Brothers, E.; Kudin, K. N.; Staroverov, V. N.; Keith, T.; Kobayashi, R.; Normand, J.; Raghavachari, K.; Rendell, A.; Burant, J. C.; Iyengar, S. S.; Tomasi, J.; Cossi, M.; Millam, J. M.; Klene, M.; Adamo, C.; Cammi, R.; Ochterski, J. W.; Martin, R. L.; Morokuma, K.; Farkas, O.; Foresman, J. B.; Fox, D. J. *Gaussian 09*, revision D.01; Gaussian, Inc.: Wallingford CT, 2016.
(40) Pal, A.; Roy, S.; Kumar, A.; Mahmood, S.; Khodapanah, N.; Thomas, S.; Agatemor, C.; Ghosal, K. Physicochemical Characterization, Molecular Docking, and *In Vitro* Dissolution of Glimepiride−Captisol Inclusion Complexes. *ACS Omega* **2020**, *5*, 19968−19977.
(41) Roy, N.; Bomzan, P.; Ghosh, B.; Roy, M. N. A Combined Experimental and Theoretical Study on p-Sulfonatothiacalix [4] arene Encapsulated Sulisobenzone. *New J. Chem.* **2023**, *47*, 1045−1049.
(42) Dallakyan, S.; Olson, A. J. Small-molecule library screening by docking with PyRx. *Chem. Biol.* **2015**, 243−250.
(43) Bauer, A. W.; Kirby, W.M.M.; Scherris, J. C.; Turck, M. Antibiotic susceptibility testing by a standardized single diffusion method. *Am. J. Clin. Pathol.* **1966**, *45*, 493−496.

https://doi.org/10.1021/acsomega.3c02783
ACS Omega 2023, 8, 29388−29400

(44) Mosmann, T. Rapid colorimetric assay for cellular growth and survival: application to proliferation and cytotoxicity assays. *J. Immunol. Methods* **1983**, *65*, 55−63.
(45) Denizot, F.; Lang, R. Rapid colorimetric assay for cell growth and survival, modifications to the tetrazolium dye procedure giving improved sensitivity and reliability. *J. Immunol. Methods* **1986**, *89*, 271−277.
(46) Cramer, F.; Saenger, W.; Spatz, H-Ch. Inclusion Compounds. XIX 1a. The formation of inclusion compounds of α-cyclodextrin in aqueous solutions, Thermodynamics and kinetics. *J. Am. Chem. Soc.* **1967**, *89*, 14−20.
(47) Alshaer, W.; Zraikat, M.; Amer, A.; Nsairat, H.; Lafi, Z.; Alqudah, D. A.; Al Qadi, E.; Alsheleh, T.; Odeh, F.; Odeh, F.; Alkaraki, A.; Zihlif, M.; Zihlif, M.; Bustanji, Y.; Fattal, E.; Awidi, A. Encapsulation of echinomycin in cyclodextrin inclusion complexes into liposomes: *In vitro* antiproliferative and anti-invasive activity in glioblastoma. *RSC Adv.* **2019**, *9*, 30976−30988.
(48) Benkovics, G.; Afonso, D.; Darcsi, A.; Béni, S.; Conoci, S.; Fenyvesi, É.; Szente, L.; Malanga, M.; Sortino, S. Novel β-cyclodextrin−Eosin conjugates. *Beilstein J. Org. Chem.* **2017**, *13*, 543−551.
(49) Rani, D.; Sethi, A.; Kaur, K.; Agarwal, J. Ultrasonication-assisted synthesis of a D -glucosamine-based β-CD inclusion complex and its application as an aqueous heterogeneous organocatalytic system. *J. Org. Chem.* **2020**, *85*, 9548−9557.
(50) de Araujo, D. R.; Tsuneda, S. S.; Cereda, C. M. S.; Carvalho, F. D. G. F.; Preté, P. S. C.; Fernandes, S. A.; Yokaichiya, F.; Franco, M. K. K. D.; Mazzaro, I.; de Fraceto, L. F. A.; Braga, F. A.; de Paula, E. Development and pharmacological evaluation of ropivacaine-2-hydroxypropyl-β-cyclodextrin inclusion complex. *Eur. J. Pharm. Sci.* **2008**, *33*, 60.
(51) BIOVIA Dassault Systèmes. In *Discovery Studio Visualizer, v21.1.0.20298*; Dassault Systèmes: San Diego, 2020.
(52) Caddeo, C.; Manconi, M.; Valenti, D.; Pini, E.; Sinico, C. Photostability and solubility improvement of β-cyclodextrin-included tretinoin. *J. Incl. Phenom. Macrocyclic Chem.* **2007**, *59*, 293−300.
(53) Ghosh, B.; Roy, N.; Roy, D.; Mandal, S.; Ali, S.; Bomzan, P.; Roy, K.; Roy, M. N. An extensive investigation on supramolecular assembly of a drug (MEP) with β-CD for innovative applications. *J. Mol. Liq.* **2021**, *344*, No. 117977.
(54) Ren, L.; Wang, J.; Chen, G. Preparation, optimization of the inclusion complex of glaucocalyxin A with sulfobutylether-β-cyclodextrin and antitumor study. *Drug Delivery* **2019**, *26*, 309−317.
(55) Rai, V.; Kumar, A.; Das, V.; Ghosh, S. Evaluation of chemical constituents and in vitro antimicrobial, antioxidant and cytotoxicity potential of rhizome of *Astilbe rivularis* (Bodho-okhati), an indigenous medicinal plant from Eastern Himalayan region of India. *BMC Complementary Altern. Med.* **2019**, *19*, No. 200.
(56) Loftsson, T. Drug permeation through biomembranes: cyclodextrins and the unstirred water layer. *Die Pharmazie* **2012**, *67*, 363−370.
(57) Loftsson, T.; Stefánsson, E. Cyclodextrins in ocular drug delivery: theoretical basis with dexamethasone as a sample drug. *J. Drug Delivery Sci. Technol.* **2007**, *17*, 3−9.
(58) Dahan, A.; Miller, J. M.; Hoffman, A.; Amidon, G. E.; Amidon, G. L. The solubility-permeability interplay in using cyclodextrins as pharmaceutical solubilizers: mechanistic modeling and application to progesterone. *J. Pharm. Sci.* **2010**, *99*, 2739−2749.
(59) Sugano, K. Possible reduction of effective thickness of intestinal unstirred water layer by particle drifting effect. *Int. J. Pharm.* **2010**, *387*, 103−109.
(60) Loftsson, T.; Brewster, M. E. Pharmaceutical applications of cyclodextrins: effects on drug permeation through biological membranes. *J. Pharm. Pharmacol.* **2011**, *63*, 1119−1135.
(61) Bhat, S.; Muthunatarajan, S.; Mulki, S. S.; Bhat, K. A.; Kotian, K. H. Bacterial Infection among Cancer Patients: Analysis of Isolates and Antibiotic Sensitivity Pattern. *Int. J. Microbiol.* **2021**, *2021*, No. 8883700.
(62) Fraceto, L. F.; Grillo, R.; Sobarzo-Sánchez, E. Cyclodextrin inclusion complexes loaded in particles as drug carrier systems. *Curr. Top. Med. Chem.* **2014**, *14*, 518−525.
(63) Aleksi, M. M.; Kapetanovi, V. An overview of the optical and electrochemical methods for detection of DNA−drug interactions. *Acta Chim. Slov.* **2014**, *61*, 555−573.
(64) Sirajuddin, M.; Ali, S.; Shah, N. A.; Khan, M. R.; Tahir, M. N. Synthesis, characterization, biological screenings and interaction with calf thymus DNA of a novel azomethine 3-((3, 5-dimethylphenylimino) methyl) benzene-1, 2-diol. *Spectrochim. Acta, Part A* **2012**, *94*, 134−142.
(65) Sirajuddin, M.; Ali, S.; Badshah, A. Drug−DNA interactions and their study by UV−Visible, fluorescence spectroscopies and cyclic voltametry. *J. Photochem. Photobiol. B: Biology* **2013**, *124*, 1−19.
(66) Galmarini, C. M.; Mackey, J. R.; Dumontet, C. Nucleoside analogues and nucleobases in cancer treatment. *Lancet Oncol.* **2002**, *3*, 415−424.
(67) Buoro, R. M.; Lopes, I. C.; Diculescu, V. C.; Serrano, S. H. P.; Lemos, L.; Oliveira-Brett, A. M. In situ evaluation of gemcitabine−DNA interaction using a DNA-electrochemical biosensor. *Bioelectrochemistry* **2014**, *99*, 40−45.
(68) Losa, R.; Sierra, M. I.; Gi′on, M. O.; Esteban, E. J.; Buesa, M. Simultaneous determination of gemcitabine di-and triphosphate in human blood mononuclear and cancer cells by RP-HPLC and UV detection. *J. Chromatogr. B* **2006**, *840*, 44−49.
(69) Moravek, Z.; Neidle, S.; Schneider, B. Protein and drug interactions in the minor groove of DNA. *Nucleic Acids Res.* **2002**, *30*, 1182−1191.
(70) Neidle, S. DNA minor-groove recognition by small molecules. *Nat. Prod. Rep.* **2001**, *18*, 291−309.

https://doi.org/10.1021/acsomega.3c02783
ACS Omega 2023, 8, 29388−29400